



## Recycling the lid: Effects of subduction and stirring on boundary layer dynamics in bottom-heated planetary mantle convection

V. Thyalan,<sup>1</sup> A. M. Jellinek,<sup>2</sup> and A. Lenardic<sup>3</sup>

Received 26 July 2006; revised 12 September 2006; accepted 26 September 2006; published 31 October 2006.

[1] The subduction and stirring of cold oceanic lithosphere governs the thermal regime of the Earth's mantle. Whether upwelling mantle plumes are transient isoviscous thermals or long-lived low viscosity plumes depends on the magnitude of the resulting temperature variations in the thermal boundary layer at the base of the mantle. Previous laboratory experiments suggest that low viscosity "Earth-like" plumes occur where the hot thermal boundary layer (TBL) viscosity ratio,  $\lambda_h > O(10)$ . Here, the results from two-dimensional numerical simulations, in which subduction is either forced from above or allowed to arise naturally show that: (1) a morphologic transition from upwellings in the form of isoviscous thermals to cavity plumes occurs where  $\lambda_h \geq O(10)$  and is accompanied by a qualitative change in the temporal and spatial dynamics of the hot TBL; (2) this transition corresponds to a condition in which the velocity boundary layer (VBL) is concentrated within the basal part of the TBL for no- and free-slip boundaries; and (3) a regime in which  $\lambda_h \geq O(10)$  can only occur if the total viscosity ratio across the convecting system,  $\lambda_T \geq O(10^2)$ . Our results support a recent conjecture that low viscosity mantle plumes in the Earth are a consequence of strong mantle cooling by plate tectonics. Moreover, Earth-like plume models may be inappropriate for explaining the origin of surface features on one plate planets such as Mars or Venus. **Citation:** Thyalan, V., A. M. Jellinek, and A. Lenardic (2006), Recycling the lid: Effects of subduction and stirring on boundary layer dynamics in bottom-heated planetary mantle convection, *Geophys. Res. Lett.*, 33, L20318, doi:10.1029/2006GL027668.

### 1. Introduction and Motivation

[2] Identifying key influences of plate subduction and large-scale mantle stirring on the structure and dynamics of the thermal boundary layer at the core-mantle boundary (CMB) is important for understanding the style and heat transfer properties of mantle convection in the Earth [Sleep, 1992; Labrosse, 2002; Gonnermann *et al.*, 2004]. Jellinek and Manga [2004] argue that the hot, narrow, low viscosity mantle plumes inferred to give rise to hotspot volcanism on Earth are a direct consequence of the strong mantle cooling that is characteristic of a plate tectonic or "active-lid" mode of mantle convection [Moresi and Solomatov, 1998]. If

correct, this argument implies that the application of "Earth-like" mantle plume models to one plate planets may be inappropriate because the comparatively smaller temperature variations in the hot thermal boundary layer characteristic of a "stagnant lid" mode of mantle convection are insufficient to produce this class of upwelling structure. Consequently, explaining the origin of surface features such as the Atla and Beta highland regions on Venus or the Tharsis bulge on Mars with an "Earth-like" plume model, although a conventional view [e.g., Schubert *et al.*, 2001], is potentially problematic.

[3] In addition to investigating controls on the structure of the hot thermal boundary layer in the active lid regime, a central motivation for this study is to identify the conditions in which subduction and mantle stirring can lead to the formation of low-viscosity plumes analogous to those inferred for the Earth. In a recent paper, Jellinek *et al.* [2003] (JGR03 from here on) use analog laboratory experiments to study the influence of a large-scale flow imposed from above on basally-heated mantle convection. From measurements of local heat flux JGR03 infer two flow regimes depending on the ratio,  $\lambda_h$ , of the viscosity of the fluid interior,  $\mu_i$ , to the viscosity of fluid in contact with the hot boundary,  $\mu_h$  and the velocity of the large-scale flow. Where  $\lambda_h < O(10)$ , vertical velocity gradients growing in response to the interaction between imposed lateral motions and the rigid hot bottom boundary (i.e., the velocity boundary layer, VBL) extend from the system base, through the conductive thermal boundary layer (TBL), and into the overlying convecting interior. Convective upwellings here are intermittent, nearly isoviscous "thermals". In contrast, where  $\lambda_h > O(10)$  it is argued that the VBL is confined to lowest viscosity basal part of the hot thermal boundary layer and upwellings are "cavity plumes" with large heads and narrow trailing conduits [Olson and Singer, 1985]. A more complete discussion of the distinction between cavity plumes and thermals is given by Jellinek and Manga [2004]. The notation " $O()$ " indicates "order" of magnitude.

[4] Taken together with speculations from previous studies [e.g., Loper and Stacey, 1983; Lenardic and Kaula, 1994; Sleep, 2004] the results of JGR03 support a hypothesis that the morphologic transition from thermals to cavity plumes occurs where the VBL becomes thinner than the TBL (Figure 1). That is, in contrast to thermals, which form by the breakup and detachment of the full thickness of the TBL, cavity plumes form predominantly by lateral flow of the lowest viscosity material into nascent convective instabilities. However, the experiments in JGR03 have a number of practical limitations that restrict their application to mantle convection driven by core-cooling. First, the large-scale flow is forced from above rather than driven by buoyancy and viscous forces arising naturally in the system. Second, the

<sup>1</sup>Department of Earth Atmosphere and Space Sciences, Massachusetts Institute of Technology, Cambridge, Massachusetts, USA.

<sup>2</sup>Department of Earth and Ocean Sciences, University of British Columbia, Vancouver, British Columbia, Canada.

<sup>3</sup>Department of Geology and Geophysics, Rice University, Houston, Texas, USA.

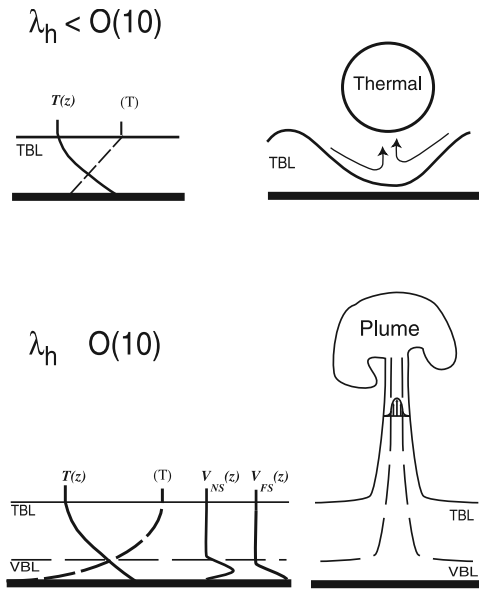


**Figure 1.** Cartoons showing the structure of the thermal boundary layer and flow regime leading to (top) hot rising thermals and (bottom) low viscosity cavity plumes. Notation is defined in the text.

experiments are transient, heated from below more strongly than they are cooled from above. For a given stirring rate a narrow range of  $\lambda_h$  conditions is explored as a consequence of the system heating up over time. By design this approach is a way to isolate the influence of large-scale flow on the hot boundary layer. Additional thermal and mechanical effects of a rheologically-complex cold thermal boundary layer, which are an integral part of mantle convection, are not considered. Finally, the floor of the tank is a rigid boundary. Although such a boundary condition may be appropriate for Venus (there are no constraints on whether the core of Venus is solid or liquid), it is inappropriate for the CMB of the Earth.

[5] A technical aim of this work is to establish the extent to which the proposed transition in boundary layer structure and convective regime at  $\lambda_h \sim O(10)$  is a general feature of mantle convection in an active-lid regime. We use two-dimensional numerical simulations conducted under thermally steady-state conditions to characterize the effects of top cooling, and the associated viscosity variations in the cold boundary layer, and free- versus no-slip basal boundary conditions. Simulations are performed using both a fixed velocity upper boundary condition, as done in the experiments, as well as under conditions in which subduction can arise naturally [Moresi and Solomatov, 1998].

## 2. Numerical Simulations

[6] We use the CITCOM finite element code to solve the equations of convection in the limit of infinite Prandtl Number. Numerical simulations are run to statistically steady-state conditions and the accuracy of the code is tested against standard benchmark solutions [Blackenbach et al., 1989]. Convergence testing is also performed to assure that simulations are well resolved. Simulations are two-dimensional (2D) and are performed using  $64 \times 64$ ,  $96 \times 96$ , and  $128 \times 128$  meshes over any  $1 \times 1$  patch of the

domain. The difference in system outputs from the lower to the higher density meshes indicated that discretization errors were less than 3% for all results reported. Most importantly, we confirm that general trends we report below are not influenced by mesh errors.

[7] The non-dimensional system of equations with the Boussinesq approximation is:

$$\partial_i u_i = 0 \quad (1)$$

$$\partial_j [2\mu(T)\epsilon_{ij}] = \partial_i p + Ra_h T \hat{k} \quad (2)$$

$$\partial_t T + u_i \partial_i T = \partial_i^2 T \quad (3)$$

$$\rho = [1 - \alpha(T - T_0)] \quad (4)$$

where  $Ra_h = \rho_0 g \alpha \Delta T D^3 / \mu_h \kappa$  is the Rayleigh number. Here,  $\mu_h$  is the viscosity,  $u_i$  is the velocity vector,  $\mu(T)$  is the viscosity,  $T$  is temperature,  $\epsilon_{ij}$  is the strain rate tensor,  $p$  is pressure,  $\hat{k}$  is the vertical unit vector,  $\rho$  is the density,  $\alpha$  is the coefficient of thermal expansion,  $g$  is the acceleration due to gravity,  $\Delta T$  is the temperature difference across the layer,  $D$  is the layer depth, and  $\kappa$  is thermal diffusivity. Subscripts of zero indicate reference values and subscripts  $c$  and  $h$  denote quantities measured at the “cold, and “hot” boundaries. Equations (1–3) are the continuity, momentum and energy equations for incompressible flow. Equation (4) is the linearized equation of state. In addition, assuming that the mantle deforms in the diffusion creep limit we apply the reasonable approximation for the viscosity law

$$\mu = A \exp(-\theta T), \quad (5)$$

where  $\theta$  is the activation energy and  $A$  is a constant.

[8] To broaden the parameter space of JGR03 we perform two series of simulations. In an initial “forced convection setup” carried out in a  $1 \times 1$  cartesian domain we fix  $Ra_h = 10^8$  and apply a fixed velocity upper boundary condition and explore the additional consequences of strong top cooling, free- and no-slip sidewall and basal boundary conditions. Variations in the magnitude of the temperature dependence of the viscosity (equation (5)) are conveniently expressed in terms of their effect on the total viscosity variation across the system,  $\lambda_T = \mu_c / \mu_h$ , and are also investigated. We note that in the absence of forced subduction where  $\lambda_T > O(10^3)$  the flow is expected to be in the stagnant lid regime [Solomatov and Moresi, 2000]. The applied surface velocity,  $V_s$  is expressed non-dimensionally as a Peclet number,  $Pe = VD/\kappa$ . This set of calculations has two goals, which are to identify whether a transition from thermals to cavity plumes occurs when  $\lambda_T > O(10)$  and also to further characterize the spatial and temporal dynamics of the thermal boundary layer.

[9] In a second set of “free convection” simulations we investigate whether a similar transition in flow regime emerges if subduction and large-scale stirring of the cold boundary layer arise naturally in the system. Following Moresi and Solomatov [1998] we apply a viscoplastic mantle rheology that can allow for an active-lid mode of convection and for an internal mantle viscosity that depends strongly on

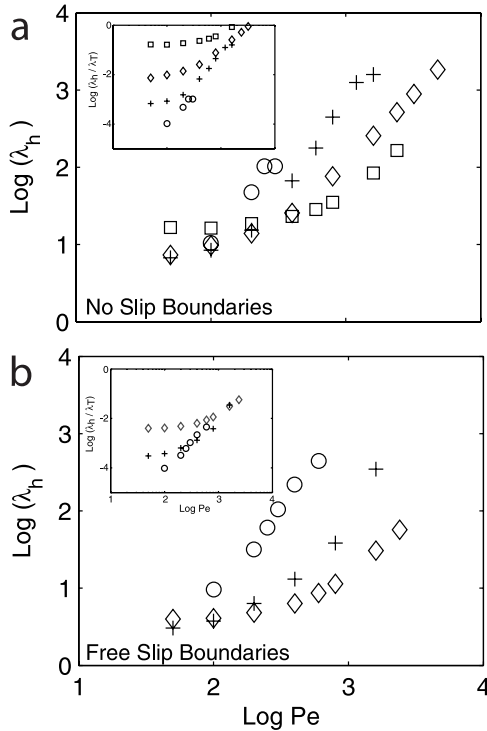


**Figure 2.** Plots showing  $\lambda_h$  and (insets) the ratio  $\lambda_h/\lambda_T$  as a function of  $Pe$  and  $\lambda_T$  for (a) no-slip and (b) free-slip boundaries. Circles:  $\lambda - T = 10^5$ ; Plus:  $\lambda_T = 10^4$ ; Diamonds:  $\lambda_T = 10^3$ ; Squares:  $\lambda_T = 10^2$ .

temperature. That is, for convective stresses below a critical yield stress,  $\tau_y$ , the rheology is given by equation (5). For stresses above  $\tau_y$ , however, the rheology is nonlinear and the effective viscosity is given by  $\mu_{plastic} = \tau_y/I$ , where  $I$  is the second strain-rate invariant. Where stresses exceed  $\tau_y$ , strain is localized in narrow shear zones and the stagnant lid fails resulting in active-lid convection. A particular utility of this formulation is that subduction and stirring of the cold boundary layer can occur without doing external work on the system, the dissipation of which may influence the temperature and, thus, viscosity variations in the hot thermal boundary layer. Here, we perform calculations only in the active-lid regime and for a constant  $\tau_y$ . For a given  $Ra_h$  and system aspect ratio we vary  $\lambda_T$  in order to sweep through a broad range of  $\lambda_h$  conditions. In these runs we fix the aspect ratio to be 1 for runs in which  $Ra_h = 10^8$ , and 1–4 for lower

$Ra_h$ . We note that  $Ra_h > 10^6$  in all simulations. The boundary conditions for all cases are constant temperature, free slip top and bottom. Side boundary conditions are reflecting for lower aspect ratios and either reflecting or wrap-around for larger aspect ratios. We focus on basal boundary layer structure and map the ratio,  $\Delta$ , of the horizontally-averaged thickness of the VBL to the horizontally-averaged thickness of the TBL as a function of  $\lambda_h$ . Following JGR03, our goal is to determine whether  $\Delta < 1$  where  $\lambda_h > O(10)$  under these conditions.

### 3. Results

#### 3.1. Forced Convection Cases

[10] The main effect of the imposed stirring is to deliver cold material to the base of the system. At steady-state, the magnitude of the cooling carried by the large-scale flow thus governs the temperature difference from the interior to the hot boundary, and through equation (5),  $\lambda_h$ . Figures 2a and 2b show that for a given  $\lambda_T$ ,  $\lambda_h$  increases with  $Pe$ , consistent with their being less time for descending cold material to equilibrate thermally with the interior as  $Pe$  becomes large. However, the rate of increase of  $\lambda_h$  with  $Pe$  increases abruptly for all  $\lambda_T \geq 100$  when  $\lambda_h \geq O(10)$  for both no- and free-slip boundaries. In addition, the rate of increase appears to be greater for no-slip boundaries: Inset plots show that where  $\lambda_h > O(10)$  the ratio  $\lambda_h/\lambda_T \propto Pe^\alpha$ , where  $\alpha \approx 1.5$  and  $\alpha \approx 2$  for free- and no-slip boundaries, respectively.

[11] The spatial and temporal dynamics of the hot boundary layer also depend on whether  $\lambda_h > O(10)$ . Figure 3 shows time series of the average basal heat flux,  $Nu$ , and snapshots from simulations with no-slip basal and sidewall boundaries. The lower time series and image on the left are from a simulation in which  $\lambda_h < O(10)$ . Hot thermal boundary layer fluid coupled to the rigid boundary is overrun by the spreading cold material, forming a thin “squeeze layer”. The thickness of the squeeze layer increases monotonically downstream until it is sufficiently thick to undergo convective instabilities leading to the intermittent formation and rise of nearly isoviscous thermals. The upper time series and the image on the right side is characteristic of flows in which  $\lambda_h > O(10)$ , which is observed only when  $\lambda_T > 10^2$ . In addition to a higher average  $Nu$ , resulting from larger temperature differences across the hot thermal boundary layer, the time series show quasi-periodic convective instabilities (i.e., “bursts”) of buoyant squeeze layer fluid. The excess temperatures carried by these upwellings are larger than for thermals and they take the form of low

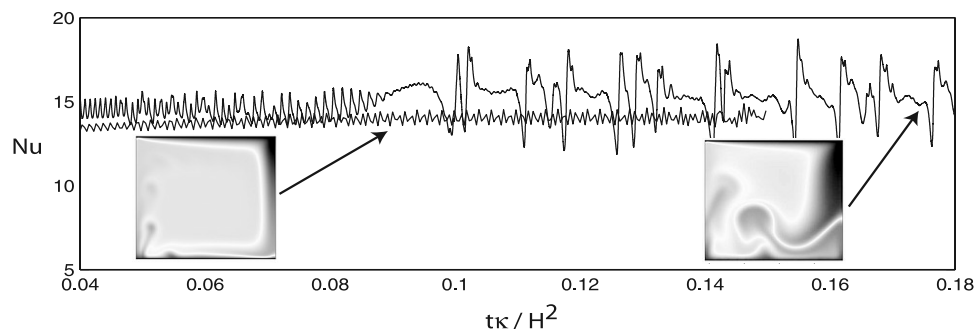


**Figure 3.** Time series of heat flux and snapshots. (bottom time series, left image)  $Pe = 400$  and  $\lambda_T = 10^4$ ; (top time series, right image)  $Pe = 600$ , for  $\lambda_T = 10^4$ .

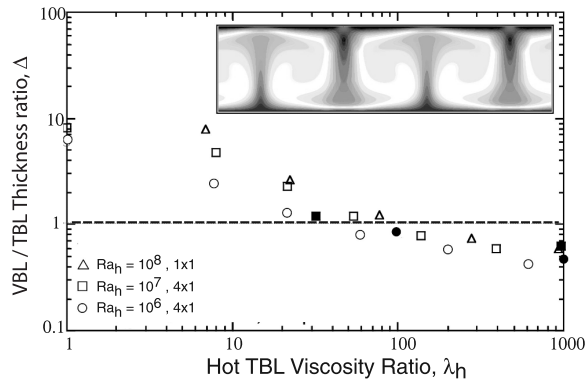


**Figure 4.** The VBL/TBL thickness ratio,  $\Delta$  as a function of  $\lambda_h$ .

viscosity cavity plumes, analogous to those observed in laboratory studies. We are insufficiently able to resolve TBLs in flows with very large  $\lambda_T$  to establish the bursting period over a large parameter space. Qualitatively, however, the period increases with  $\lambda_T$  and  $Pe$ . For given  $\lambda_T$  similar bursting is observed with approximately the same frequency characteristics in large aspect ratio simulations (aspect ratios of 4) as well as in simulations with free-slip, and periodic boundaries. Thus, this feature is not a consequence of phenomena such as corner flows that can arise in the presence of no-slip boundaries. It is, however, worth noting that the effect is more pronounced for the no-slip cases and that this difference is likely a consequence of an enhanced squeeze layer thickness due to the no-slip basal boundary condition.

### 3.2. Free Convection Cases: Subduction and Mantle Stirring

[12] The results from simulations of active-lid convection in a viscoplastic mantle are shown in Figure 4. The boundary layer thickness ratio  $\Delta$  is plotted against  $\lambda_h$  for a range of  $Ra_h$ . The thicknesses of the VBL and TBL are defined as the positions above the bottom boundary at which the horizontally-averaged rms vertical velocity and temperature profiles reaches  $\approx 90\%$  of the value for the internal core of the modeling domain. Velocity and temperature profiles are averaged over several system overturn times so that boundary layer thickness reported represent both spatial and temporal averages. When  $\lambda_h \geq O(10)$  the velocity boundary layer is thinner than the hot thermal boundary layer over a wide range of conditions. In addition, by virtue of the setup of these calculations the interior temperature in the active-lid regime is the mean of the two boundaries. Consequently we find that  $\lambda_h \approx \lambda_T^{1/2}$ , which is expected from the viscosity law given by equation (5). Thus, a further result, that is consistent with the forced convection simulations is that in order for  $\lambda_h \geq O(10)$  the total viscosity ratio  $\lambda_T \geq O(10^2)$ .

## 4. Discussion and Applications to Mantle Convection

[13] The combined numerical results support and generalize to a larger parameter space two inferences from the laboratory experiments of JGR03. First, the forced convection runs show that a transition from conditions leading to thermals to those leading to cavity plumes occurs where

$\lambda_h \geq O(10)$  and that such a transition is only observed if the total viscosity ratio  $\lambda_T \geq O(10^2)$ . Second, the free convection results show that such a transition in flow regime is a direct result of the VBL becoming thinner than the TBL, which also can only occur if  $\lambda_T \geq O(10^2)$ . Both suites of simulations taken together with the laboratory results in JGR03 provide the first direct support for the long-standing hypothesis [Loper and Stacey, 1983] that the transition from thermals to cavity plumes occurs because the VBL becomes thinner than the TBL. In a fluid with a strongly temperature-dependent viscosity this transition is governed entirely by the magnitude of the local temperature variations in the TBL. One caveat is that in contrast to laboratory experiments hot upwellings in our simulations are 2D sheets. However, the good agreement with the laboratory experiments under similar conditions suggests that the transition in TBL structure at  $\lambda_h > O(10)$ , which gives rise to the change from thermals to plumes, is not sensitive to the 2D geometry of the calculations. A full suite of 3D calculations would be required to make this conclusion stronger but is beyond the scope of this work.

[14] A second noteworthy result (Figure 3) is that the temporal and spatial dynamics of the thermal boundary layer are markedly different depending on whether  $\lambda_h > O(10)$ . Cavity plume “bursts” with a period that apparently increases with both  $\lambda_T$  and  $Pe$  are a characteristic feature of flows in which  $\lambda_h > O(10)$ . This feature probably reflects the changing condition for marginal stability arising in response to large vertical and lateral temperature and viscosity variations, and also to the presence of vertical shear and the downstream advection of buoyant hot boundary layer fluid. This regime may be influenced by the buoyancy flux carried by the upwellings and thus may also be sensitive to whether calculations are done in 2D or 3D geometries.

[15] Our results have implications for active lid mantle convection on the Earth as well as for comparison with one-plate planets and moons in the stagnant lid regime. However, one explicit difference between planetary mantles and our models that must first be discussed is the additional presence of volumetric internal heating, which we do not include in the calculations. Depending on its magnitude, the major effect of internal heating on the hot TBL is to reduce the temperature difference from the mantle to the hot boundary [Lenardic and Kaula, 1994; Labrosse, 2002]. As noted above, the key physics governing the structure and dynamics of the TBL is the magnitude of the temperature variations arising due to subduction and not the absolute temperature of the system. Thus, although additional internal heating will modulate such variations it will not influence whether a transition in TBL structure occurs where  $\lambda_h \sim O(10)$ . The higher mean interior temperature implies that the transition will occur for a larger  $\lambda_T$  than found in our simulations (but still for  $\lambda_T \ll 10^6$ , which is taken typically as a lower bound for planetary mantles).

[16] In a stagnant lid regime mantle upwellings are expected to be nearly isoviscous thermals [Solomatov and Moresi, 2000; Labrosse, 2002], thus carrying an excess temperature that is much less than the  $\geq 200^\circ\text{C}$  typically inferred for plumes in the Earth, which implies  $\lambda_h \geq 10^2$ . Our work shows that subduction and stirring of the stagnant lid are required to produce large Earth-like temperature variations—particularly in the presence of internal heating. This

result supports a conjecture outlined initially by Nataf [1991] and explored in subsequent studies [Lenardic and Kaula, 1994; Jellinek et al., 2002; Jellinek and Manga, 2004] that hot, low viscosity mantle plumes in the Earth are an inevitable consequence of subduction and plate tectonics. Finally, the thermal regime in which low viscosity “Earth-like” plumes may form is restrictive: The conventional application of such plume models to explaining the origin of the Atla and Beta highlands regions on Venus and to the origin of the Tharsis bulge on Mars, is not consistent with a stagnant-lid regime of mantle convection. However, It should be noted that long-lived isoviscous and columnar upwellings may occur if  $Ra_h$  is low [Olson and Singer, 1985; Weeraratne and Manga, 1998]. Thus, our conclusions must also be regarded with caution.

[17] **Acknowledgments.** Comments from S. King and R. Lenardic and one anonymous reviewer improved this manuscript. V. T. thanks H. and M. Thayalan for support. A. M. J. and V. T. have been supported by NSERC and the Canadian Institute for Advanced Research during completion of this study. This work has been supported also by NSF grant EAR-0448871 to A. L.

## References

- Blackenbach, A., et al. (1989), A benchmark comparison for mantle convection codes, *Geophys. J. Int.*, *98*, 23–38.
- Gonnermann, H. M., A. M. Jellinek, M. A. Richards, and M. Manga (2004), Modulation of mantle plumes and heat flow at the core-mantle boundary by plate-scale flow: Results from laboratory experiments, *Earth Planet. Sci. Lett.*, *226*, 53–67.
- Jellinek, A. M., and M. Manga (2004), Links between long-lived hot spots, mantle plumes,  $D''$ , and plate tectonics, *Rev. Geophys.*, *42*, RG3002, doi:10.1029/2003RG000144.
- Jellinek, A. M., A. Lenardic, and M. Manga (2002), The influence of interior mantle temperature on the structure of plumes: Heads for Venus, tails for the Earth, *Geophys. Res. Lett.*, *29*(11), 1532, doi:10.1029/2001GL014624.
- Jellinek, A. M., H. M. Gonnermann, and M. A. Richards (2003), Plume capture by divergent plate motions: Implications for the distribution of hotspots, geochemistry of mid-ocean ridge basalts, and estimated of the heat flux at the core-mantle boundary, *Earth Planet. Sci. Lett.*, *205*, 361–378.
- Labrosse, S. (2002), Hotspots, mantle plumes and core heat loss, *Earth Planet. Sci. Lett.*, *199*, 147–156.
- Lenardic, A., and W. M. Kaula (1994), Tectonic plates,  $D''$  thermal structure, and the nature of mantle plumes, *J. Geophys. Res.*, *99*, 15,697–15,708.
- Loper, D. E., and F. D. Stacey (1983), The dynamical and thermal structure of deep mantle plumes, *Phys. Earth Planet. Inter.*, *33*, 304–317.
- Moresi, L.-N., and V. S. Solomatov (1998), Mantle convection with a brittle lithosphere: Thoughts on the global tectonic style of the Earth and Venus, *Geophys. J.*, *133*, 669–682.
- Nataf, H.-C. (1991), Mantle convection, plates, and hotspots, *Tectonophysics*, *187*, 361–377.
- Olson, P., and H. Singer (1985), Creeping plumes, *J. Fluid Mech*, *158*, 511–535.
- Schubert, J.-G., D. L. Turcotte, and P. Olson (2001), *Mantle Convection in the Earth and Planets*, 940 pp., Cambridge Univ. Press, New York.
- Sleep, N. H. (1992), Time dependence of mantle plumes: Some simple theory, *J. Geophys. Res.*, *97*, 20,007–20,019.
- Sleep, N. H. (2004), Thermal haloes around plume tails, *Geophys. J. Int.*, *156*, 359–362.
- Solomatov, V. S., and L.-N. Moresi (2000), Scaling of time-dependent stagnant lid convection: Application to small-scale convection on the Earth and other terrestrial planets, *J. Geophys. Res.*, *105*, 21,795–21,818.
- Weeraratne, D., and M. Manga (1998), Transitions in the style of mantle convection, *Earth Planet. Sci. Lett.*, *160*, 563–568.
- A. M. Jellinek, Department of Earth and Ocean Sciences, University of British Columbia, 6339 Stores Road, Vancouver, BC, Canada M5S 1A7. (mjellinek@eos.ubc.ca)
- A. Lenardic, Department of Geology and Geophysics, William March Rice University, Houston, TX 77001, USA. (adrian@rice.edu)
- V. Thayalan, Department of Earth Atmosphere and Space Sciences, Massachusetts Institute of Technology, Cambridge, MA 02139, USA. (vidt@MIT.edu)